Deutsche Hydrographische Zeitschrift
German Journal of Hydrography
Volume 51 (1999) Number 1

ISSN 0012-0308

Does Microseisms in Hamburg (Germany) Reflect the Wave Climate in the North Atlantic?

H.-H. ESSEN, J. KLUSSMANN, R. HERBER, I. GREVEMEYER

Summary

The possibility of monitoring climate variability on decadal scales by means of microseisms is investigated. For this purpose, digital microseismic data from Hamburg (Germany) of the six winters 1992/93 to 1997/98 are compared with model ocean-wave fields of the North Atlantic. A correlation coefficient of about $r = 0.7$ was found between the linear ocean-wave amplitude at the Norwegian coast and the square-root of the microseismic amplitude. Considering monthly means of the energy of both ocean waves and microseisms the correlation exceeds $r = 0.8$ in special areas. A correlation coefficient of $r = 0.6$ was found between the monthly winter index of the North Atlantic Oscillation (NAO) and the respectively averaged microseismic energy. Encouraged by these results, further investigations are planned for analysing earlier microseisms which has been recorded in Hamburg since 1905.

Spiegelt die in Hamburg gemessene Mikroseismik das Wellenklima im Nordatlantik wider? (Zusammenfassung)

Es wird untersucht, ob sich Klimaschwankungen mit Perioden um zehn Jahre aus Aufzeichnungen der Mikroseismik erfassen lassen. Zu diesem Zweck werden digitale Mikroseismikdaten der sechs Winter 1992/93 bis 1997/98 aus Hamburg mit Modelldaten des Seegangs im Nordatlantik verglichen. Es ergibt sich ein Korrelationskoeffizient von $r = 0,7$ zwischen den mittleren linearen Amplituden des Seegangs an der norwegischen Küste und der Wurzel aus der Amplitude der Mikroseismik. Für monatliche Mittel der Energien des Seegangs und der Mikroseismik werden in einigen Gebieten Korrelationskoeffizienten über $r = 0,8$ gefunden. Der Korrelationskoeffizient zwischen dem monatlichen Index der nordatlantischen Oszillation (NAO) und der entsprechend gemittelten Energie der Mikroseismik beträgt $r = 0,6$. Ermutigt durch diese Ergebnisse sollen historische Registrierungen der Mikroseismik analysiert werden, die in Hamburg seit 1905 vorliegen.

1 Introduction

It is generally accepted that microseisms is generated by ocean surface waves (e.g. GUTENBERG, 1924; HASSELMANN, 1963). For this reason, it can be expected that microseismic activity reflects the wave climate of the generation area within the ocean and in turn the climate itself, i.e., the frequency and strength of storm events. Climate variability on decadal scales is presently investigated in context with the index of the North Atlantic Oscillation (NAO). Correlations of the NAO index with different geophysical parameters have been reported in the literature. For example, KOSLOWSKI AND LOEWE (1994) investigated the variability of the severity of ice winters in the Baltic between 1879 and 1992. The time series of the accumulated areal ice volume is negatively correlated (correlation coefficient $r = -0.47$) with the temporally corresponding series of the NAO winter index.

For the investigation of the decadal variability, time series of climate parameters are needed which cover a period of at least 100 years. In-situ measurements of wind and waves are available but partly with insufficient accuracy and poor spatial coverage. The increase of observations within the past century can lead to the wrong conclusion of an increase of storm events (VON STORCH et al. [1995]). Because of the instruments involved and the recording at fixed stations both the NAO index and the microseisms represent relatively reliable time series. The NAO index is known since 1865, microseisms has been recorded since the beginning of the century.

The NAO index describes the difference of the sea-level air pressure between the Azores and Iceland, averaged over the winter months (ROGERS [1984]), or alternatively, between Portugal and Iceland (HURRELL [1995]). The NAO index is a simple measure of the strength of the zonal atmospheric circulation above the North Atlantic. A high index is associated with strong westerlies, a low index with weak westerlies. Thus, a positive correlation between NAO index and microseismic activity can be expected.

Microseisms is the continuous background noise on seismic records with periods between some 2 s and 20 s. Except for an interruption of 10 years (1942 – 1952) microseisms has been registrated continuously in Hamburg (Germany) since 1905. Decades ago it has already been shown that microseismic activity in Hamburg is inherently related to the ocean waves approaching the coastal waters at European continental margines off Norway and Great Britain (e.g. GUTENBERG [1924]; STROBACH [1962]). Following HASSELMANN (1963), the dominant origins of microseisms are due to nonlinear interactions between ocean surface waves (secondary microseisms), and the interaction of ocean surface waves with a sloping sea bed in coastal areas (primary microseisms). The frequencies of the primary microseisms reflect those of the generating ocean waves, while the frequencies of secondary microseisms are just the double. Microseisms as observed in Hamburg covers periods in the range 3 – 9 s, i.e., frequencies in the range 0.1 – 0.3 Hz, and can be attributed to secondary microseisms.

Seismometers provide all three components of the earth's motion. Assuming that the microseismic activity is composed by only a single mode, the two horizontal components allow an estimate of the azimuthal angle of arrival. However, due to possible refraction on the path from the generating area, this angle needs not to coincide with the direction towards the generating area (STROBACH [1962]). Recently, FRIEDRICH et al. (1998) investigated microseismic recordings of the Gräfenberg array (southern Germany) with respect to the generating areas. The recordings over four months in winter 1995/96 indicate that, for this period, the strongest source of secondary microseisms was at the north-Norwegian coast. Additional generating areas could be identified at the Atlantic coasts of Ireland and Scotland and in the Bay of Biscay.

This paper statistically investigates the dependence of microseisms on ocean-wave height and in addition, on wind and the NAO index. The main aim is to relate the microseisms to climate parameters. For the first time, maps of model sea-state data are used for comparison with microseismic recordings. Since 1992, the German Weather Service DWD (Deutscher Wetterdienst) provided digital data of the sea state on a regular grid in the North Atlantic. Also since 1992, digital registrations of the microseisms are available at the Hamburg observatory. Our analysis relies on the vertical component of the microseisms only. This restriction is reasonable with respect to the planned analysis of historic microseismic data. These are available on paper plots only, and extraction of more than amplitude and period from just one component would be too laborious.

2 Generation of secondary microseisms

Relying on the generally accepted theory, secondary microseisms is the resonant response of the earth's mantle to a pressure field generated by nonlinear interaction of ocean surface waves. This second-order pressure field was first reported by MICHE (1944) and used by LONGUETT-HIGGINS (1950) to develop a theory of the generation of microseisms. The theory was expanded further by HASSELMANN (1963). Microseisms propagate primarily as Rayleigh waves along the earth's surface. It consists of a finite number of discrete modes, of which, for a given frequency, the wavenumbers are determined by a dispersion relationship.

The resonant generation of microseisms requires that the exciting wave field contains both frequency and wavelength of microseismic waves. However, the wavelengths of microseisms (some 10 km) are much longer than those of ocean surface waves (some 100 m). By means of quadratic coupling a second-order ocean-wave field is generated. The field is composed of waves with frequencies and wavevectors, which are the sum or difference of the interacting first-order (linear) ocean waves. Long wavelengths or small wavenumbers appear, if the first-order wave field contains two wave components of about the same wavelength propagating in opposite direction. The corresponding second-order frequency is just the double of the first-order frequency.

Following HASSELMANN (1963), the spectral density of the secondary microseisms depends on the two-dimensional ocean-wave spectrum by

$$F_{ms}(\omega)= \frac{A}{R}\sum_{n=1}^{N(\omega)} T(\omega, k_n) \int f_h\left(\frac{\omega}{2}, \vartheta\right) f_h\left(\frac{\omega}{2}, \vartheta + \pi\right) d\vartheta \quad (1)$$

where F_{ms} is the variance spectrum of the vertical or horizontal microseismic displacement, A is the extent of the generation area and R the distance from this area. The transfer function T is different for vertical and horizontal displacements and is a function of the circular frequency ω and the wavenumber k_n of the microseismic mode n. The total number N of guided modes depends on frequency. The two-dimensional ocean waveheight spectrum is represented by f_h, where ϑ is the direction of the waves. Eq. (1) reveals that secondary microseisms is generated only if the ocean-wave field contains components propagating in opposite directions. The evaluation of Eq. (1) is based on the assumption that microseismic waves are dispersed seismic surface waves. Only those wavenumbers are resonantly generated, which fulfil the seismic dispersion relationship for a given frequency. Their directional distribution is isotropic. The theory predicts a two-to-one relationship between the microseismic and gravity wave frequencies. In coastal areas ocean waves popagating in opposite direction to the main field are generated by reflection. The amplitude of a reflected wave is proportional to that of the incident wave. In this case, Eq. (1) predicts a quadratic increase of the microseismic variance in terms of the ocean-wave variance.

The tranfer function T in Eq. (1) depends on the vertical layering of the sea floor, i.e. on the elastic parameters density, compressional- and shear-wave velocity as a function of depth. If these parameters are known, T can be calculated. The theory, however, assumes that the sea-floor structure is horizontally homogeneous between the generation area and the registration site. Considering Norwegian coastal waters and the city of Hamburg, this obviously does not hold. The geological structure inherently affects the propagation of microseismic waves by means of dissipation, reflection, refraction, mode-coupling etc.

3 Data

Both digital microseismic data of the Hamburg observatory and model sea-state data are available since 1992. There is little microseismic activity during the summer months. Therfore only the winter months October through March were used. The data considered spans the six winters 1992/93 to 1997/98.

3.1 Microseismic data

The geophysical observatory of the University of Hamburg (site HAM) is situated south of the river Elbe in Hamburg-Harburg (53.4650° N, 9.9247° E). Because of a high noise level in the 1–10 Hz band of the site HAM the GRSN (German Regional Seismic Network) equipment was moved to the new position called BSEG (Bad Segeberg, about 40 km NNE of Hamburg) in December 1995. This station is also maintained by the HAM observatory. The seismometer is positioned in a cave on the Anhydrit of the Kalkberg (53.9353° N, 10.3169° E). Thus, the data investigated in this paper were recorded at two different sites.

The sampling rate of the microseisms is 1 s. Mean amplitudes are computed every 3 h. These time series have been published in the WWW since 1992 (http://www.rrz.uni-hamburg.de/microseis). The amplitudes are derived from bandpass filtered registrations of 30 min duration. A 2-pole Butterworth bandpass is applied with center and corner periods (in brackets): 4 s (3 s, 5 s), 6 s (5 s, 7 s), 8 s (7 s, 9 s). Mean amplitudes are computed by determining and averaging the peak-to-trough values of the filtered time series. In general, the 4 s microseismic amplitudes are much smaller than the 6-s and 8-s amplitudes and are correlated less strongly with climate parameters (cf. Fig. 7). For this reason, the 4-s microseisms is not accounted for in the following investigations. In accordance with the sampling rate of the sea-state data, 6-hourly sampled microseismic amplitudes were used for the following investigations. Due to instrumental problems data are lacking for October–November 1993 and December 1995.

3.2 Sea-state data

The sea-state data, archived by the German Hydrographic Office BSH (Bundesamt für Seeschiffahrt und Hydropgraphie), were provided by the forecast system of the DWD, cf. BEHRENS AND SCHRADER (1994). The North Atlantic wave model is forced by the wind fields of the global atmospheric model T106. Wave forecast is based on the second generation HYPA model which combines a parametric wind-wave model with an independent calculation of swell energy for each frequency and direction interval by a ray technique, cf. GÜNTHER et al. (1979). The parametric model accounts for wind input, nonlinear interaction and dissipation. If the phase velocity of the waves exceeds the wind speed, the waves are considered as freely propagating swell.

The wave-forecast system is operational since June 1992, and provides amplitude, mean period and direction of both wind sea and swell, and in addition the wind vector. The data are available every 6 h on a grid with 150 km spacing for the North Atlantic. Our investigations are confined to the area north of 40° N and east of 30° W. Fig. 1 shows this area and displays the grid points. BEHRENS AND SCHRADER (1994) compared waveheights, as predicted by the forecast system, with values measured by buoys and retrieved from altimeter data of ERS-1 (European Remote Sensing Satellite). For both data sets, they generally found fairly good agreement, though for high waves the model tends to overestimate the waveheight. If, for example, the maximum waveheight of the buoy data is 12.0 m, the respective model value is 13.4 m.

With the exception of a few lacking data, sea-state time series extracted from the model data are complete and look reasonable. Only in February 1998, the sea state shows unreliably fast fluctua-

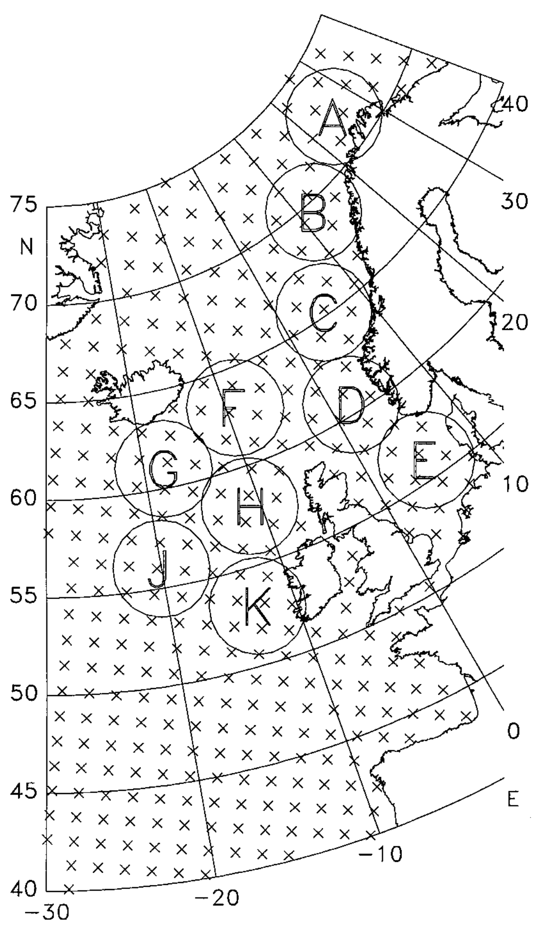

Fig. 1: Grid of the ocean-wave model. The sea state of the ten areas A- K indicated will be compared with the microseisms recorded in Hamburg.

tions. As a result, the average sea-state of this month may be underestimated. However, this possible error has only little influence on the results presented.

The following analysis makes use of total and mean amplitudes which are obtained by adding or averaging wave energies, respectively. The total waveheight h of a grid point is obtained by adding the energies of wind sea and swell, h_w and h_s. The same procedure is applied when adding 6-s and 8-s microseimic amplitudes. Analogously, mean ocean-wave amplitudes $\bar{h}$ of an area covering k grid points refer to the mean energy,

$$h = \sqrt{h^2_{\ w} + h^2_{\ s}},\ \bar{h} = \sqrt{\frac{1}{k}\sum_{i=1}^{k} h^2_{\mathrm{i}}} \qquad (2)$$

4 Correlation between microseisms and ocean surface waves

The typical propagation speed of microseismic waves is 4 kms^{-1}, suggesting that the propagation time from the Norwegian coast to Hamburg is always less than 10 min. Both the ocean surface wave field and the microseisms remain stationary over several hours. For this reason, the comparison of microseisms and generating ocean waves can refer to coinciding sample times.

Fig. 2 shows a typical ocean-wave field during a period when high microseismic amplitudes were recorded in Hamburg. Strong wind sea is propagating towards the southern coast of Norway. For periods of high microseismic activity in Hamburg, addi-

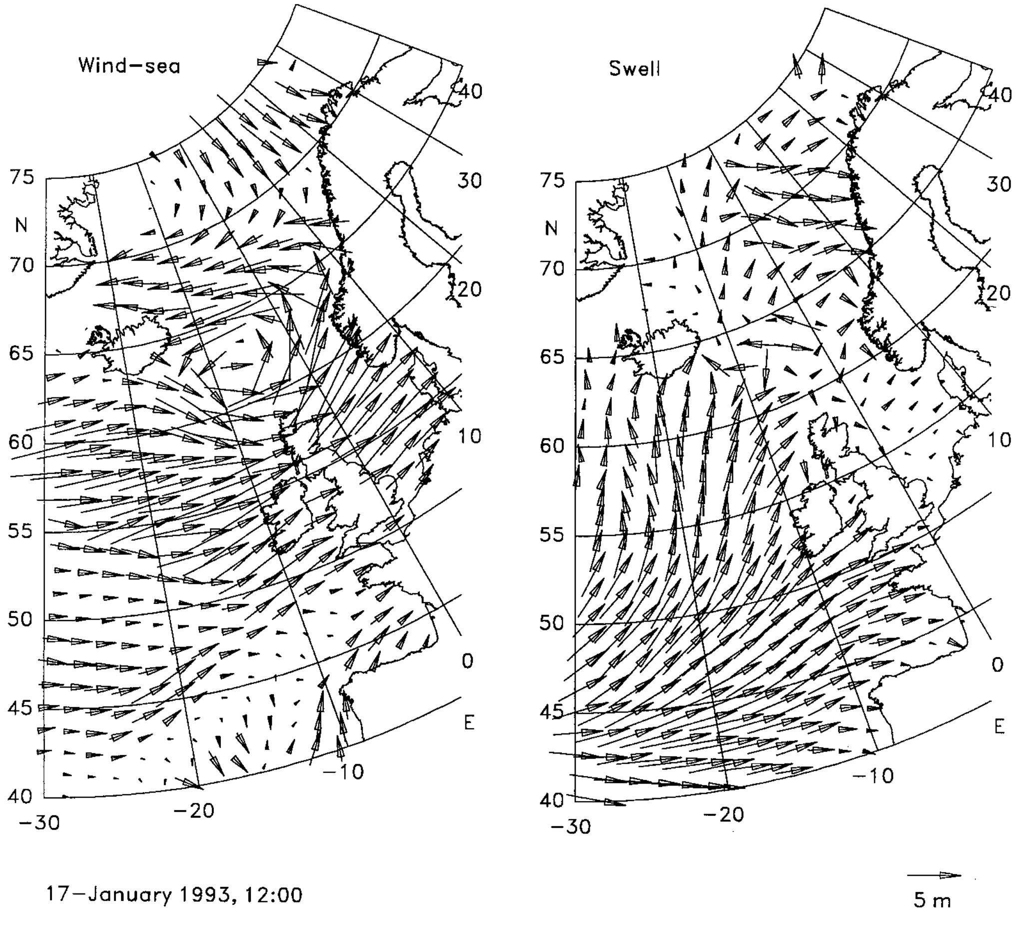

Fig. 2: Wind sea (left) and swell (right), during a period when microseismic recordings in Hamburg revealed high amplitudes, cf. Fig. 3. The length of the arrows is proportional to the mean wave height, the direction indicates the mean direction of the ocean waves.

tional 60 maps of ocean waves were visually examined. In all the cases, strong ocean waves are approaching a coast, mostly the southern Norwegian coast, but also the northern Norwegian coast and the Atlantic coasts of Scotland and Ireland. This result clearly supports earlier investigations carried out, for example, by GUTENBERG (1924), STROBACH (1962) and FRIEDRICH et al. (1998). All the areas mentioned, however, can be affected separately or simultaneously. There are less than 10 cases with sea states significantly higher at the Irish coast than at the Norwegian coast. By means of this investigation no evidence has been found for different generation areas of the 6-s and 8-s microseisms.

Three-month time series of both ocean-wave height and vertical microseismic displacement are displayed in Fig. 3. The ocean waves refer to the mean total amplitude in the five areas A – E along the Norwegian coast, i.e. the sum of wind sea and swell. Amplitudes of microseisms are displayed separately for the spectral ranges centered at 6-s and 8-s period. All the microseismic peaks coincide with ocean-wave peaks which, however, occur in different areas and with different strength.

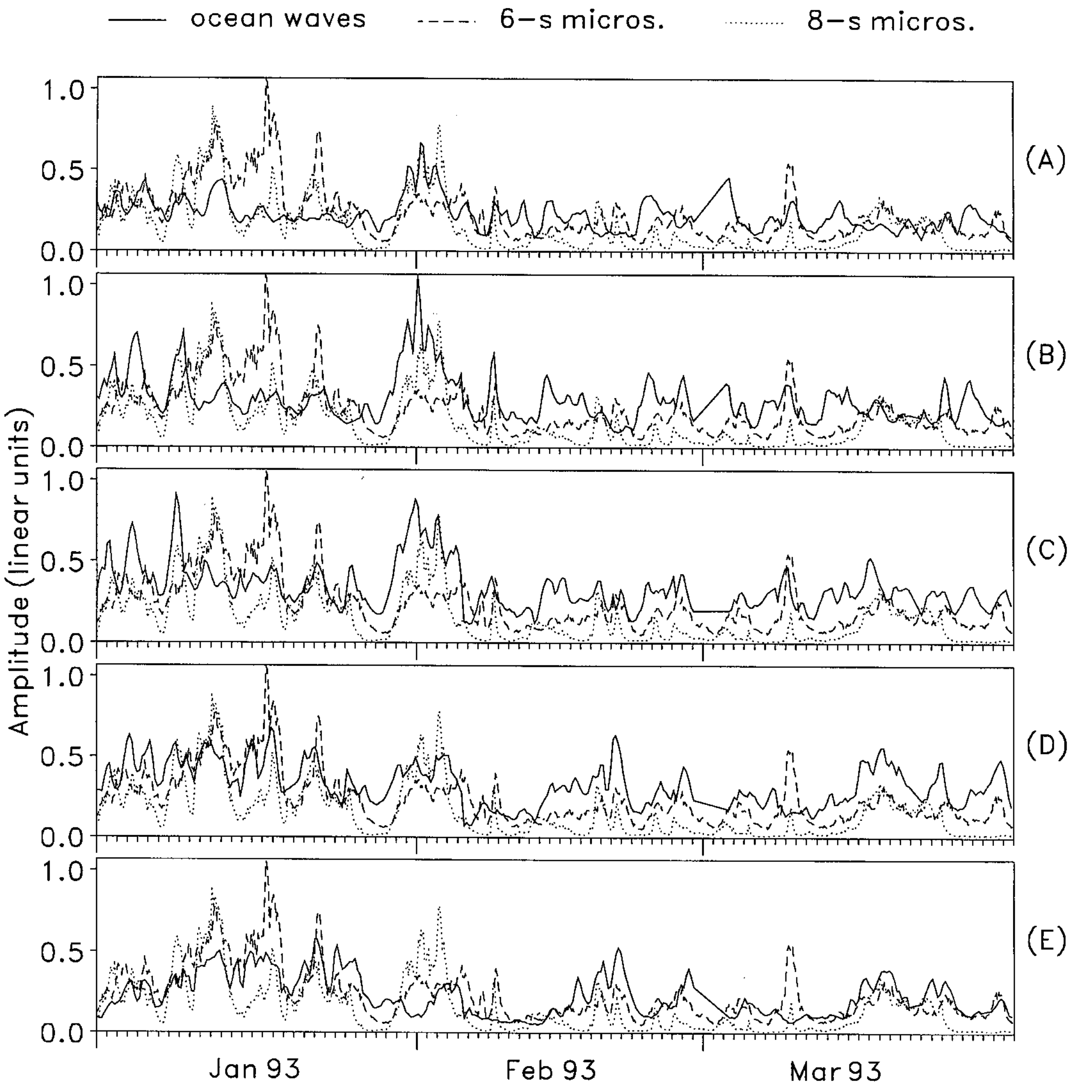

Fig. 3: Three-month time series from the five areas A-E, cf.Fig.1, of the mean amplitude of the total ocean-wave field, and the vertical amplitude of the 6-s and 8-s microseisms. The amplitude 1 refers to 15 m in the case of ocean waves and 3 μm in the case of microseisms.

In order to quantify the relation between ocean waves and microseisms, correlation coefficients were calculated. Input data are the time series of amplitudes, their square and square-root. Eq. (1) suggests that microseismic energy depends on the square of ocean-wave energy. Regarding the sample distributions of the quantities mentioned, it turns out that the linear ocean-wave amplitude shows the most normal-like (Gaussian) behaviour. With respect to the microseisms, the same holds for the square-root of the amplitude. The upper panels of Fig. 4 display the sample distributions of the mean total ocean-wave amplitude of the areas A – E and the square-root total microseismic amplitude. The data set contains all data from the six winters.

The lower panel of Fig. 4 shows the scatterplot and reveals a correlation coefficient of $r = 0.71$. As, in general, the duration of a storm event exceeds the sampling rate of 6 h not all the 3704 data pairs can assumed to be statistically independent. Nevertheless, the remaining data confirm a highly significant correlation between ocean waves and microseisms. The 95 % confidence interval of 500 independent sample pairs is approx. [0.66,0.75]. Considering the areas F – K, instead of A – E, the correlation coefficient decreases to $r = 0.65$. Replacing the amplitudes of ocean-wave height by the wind speed, correlation coefficients of $r = 0.58$ and $r = 0.51$ are found for the areas A – E and F – K, respectively. The correlation coefficient squared is the fraction of the variance that can be explained by a linear dependence of the two random variables under consideration. Thus, 50 % of the microseismic variance (in terms of the square-root amplitude) can be explained by the sea state (in terms of ocean-wave height) along the Norwegian coast.

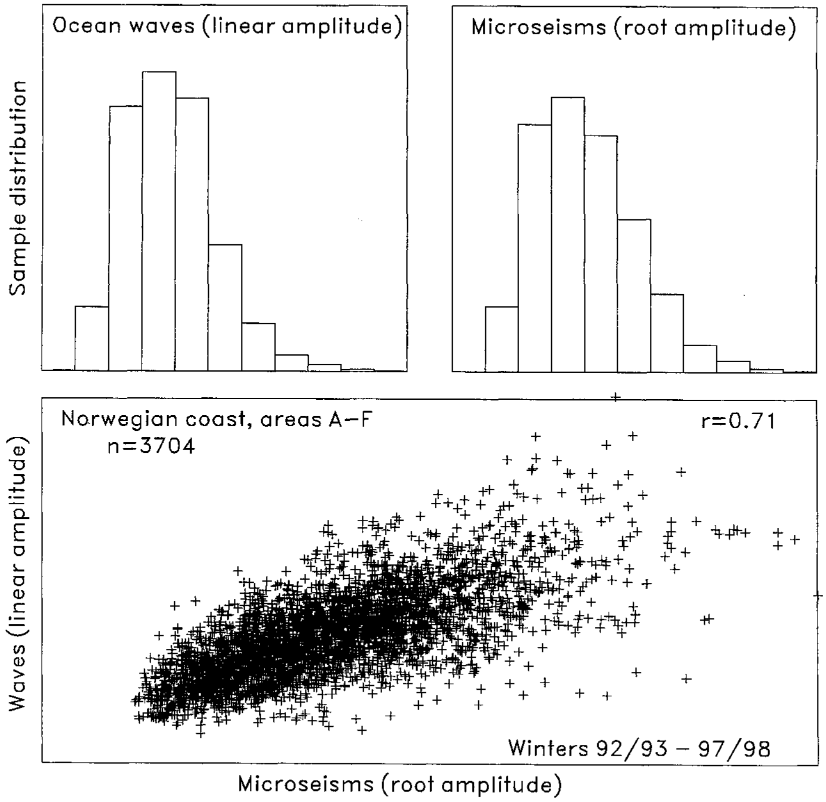

Fig. 4: Sample distributions of averaged linear total ocean-wave amplitude (upper left panel), square-root total microseismic amplitude (upper right panel), and scatterplot of linear ocean-wave amplitudes versus square-root microseismic amplitudes (lower panel). Scales range from 0 to 10 m (ocean waves) and from 0 to 1.9 $\mu m^{0.5}$ (microseisms). The data are averages over the five areas A - E along the Norwegian coast, cf. Fig. 1. Number of sample pairs n and correlation coefficient r are indicated.

Table 1 displays correlation coefficients computed separately for the ten areas A - K indicated in Fig. 1 and the six winters under investigation. The mean correlation is highest in area D (southern Norwegian coast) and second-highest in area H (Atlantic Scotish coast). Relatively low mean correlation was found for the areas A (northern Norway), G (south of Iceland), J (open North Atlantic) and E (North Sea). There is some variability from year to year. In most areas, the winter 1997/98 reveals the lowest correlation, which partly may be due to the erroneous sea-state data mentioned.

From Table 1 no clear conclusions can be drawn with respect to the generation area. One reason for this finding is the large extension of high-amplitude ocean-wave fields, which mostly cover several of the areas investigated. Another more important reason is that microseismic energy observed in Hamburg originates in different areas. These may be the areas A – K of Fig. 1 or others, e.g. the Bay of Biscay (FRIEDRICH et al. [1998]). By comparing wind sea or swell separately with either the 6-s or the 8-s microseisms, the correlation coefficients turn out to be smaller than those in Table 1.

Fig. 5 compares the monthly mean values of total energies of the ocean waves in the areas A – E with those of the microseisms. In general, microseismic peaks coincide with peaks of ocean-wave energy, preferably in area D. In order to quantify the relation between the energies, correlation coefficients are indicated. The correlation coefficients refers to all data of the six winters. The highest value of $r = 0.82$ was found for area D, but also the other areas reveal considerable correlation. The same analysis for areas F – K reveals correlation coefficients in the range $r = 0.66 – 0.80$, the highest one for area H.

The correlation coefficient is a measure of the linear dependence of two random variables. Methods for the estimation of confidence limits base on the assumption that both variables are normally distributed. A number of 36 independent sample pairs, as used in Fig. 5, and an estimated correlation coefficient of $r = 0.7$ result in a 95 % confidence interval of $r = [0.50, 0.85]$. However, the quantities compared in Fig. 5 and the following Figs. 6 and 7 are not normally distributed. Thus, the correlation coefficients presented have to be interpreted with caution.

	92/93	93/94	94/95	95/96	96/97	97/98
A	0.52	0.29	0.20	0.31	0.48	0.36
B	0.60	0.52	0.29	0.37	0.63	0.42
C	0.71	0.48	0.41	0.60	0.70	0.36
D	0.70	0.63	0.52	0.58	0.75	0.42
E	0.56	0.47	0.32	0.34	0.38	0.30
F	0.52	0.63	0.49	0.61	0.66	0.33
G	0.38	0.45	0.32	0.69	0.51	0.41
H	0.64	0.59	0.58	0.76	0.61	0.53
I	0.46	0.41	0.52	0.63	0.49	0.48
J	0.54	0.51	0.56	0.61	0.49	0.45

Tab. 1: Correlation coefficients r of linear amplitudes of the total ocean-wave field versus square-root amplitudes of the total microseisms for the six winters 1992/93 - 1997/98 in the areas A - K of Fig. 1.

Similar to Fig. 5, energies of wind sea and swell on the one hand and 6-s and 8-s microseisms on the other hand were compared. The highest correlation coefficients of $r = 0.85$ was found in the areas D and E, when comparing the 6-s microseisms with either the wind sea or the total ocean-wave field. Considering the 8-s microseisms, the correlation coefficients are considerably smaller, less than $r = 0.70$ in all the ten areas A – K under investigation. Considering swell, the highest correlation coeffient of $r = 0.74$ was found for the areas B and C. Finally, the energies of wind and microseisms were compared. The results look very similar to those between total ocean-wave field and microseisms, with correlation coefficients only about 4 % less (in the mean).

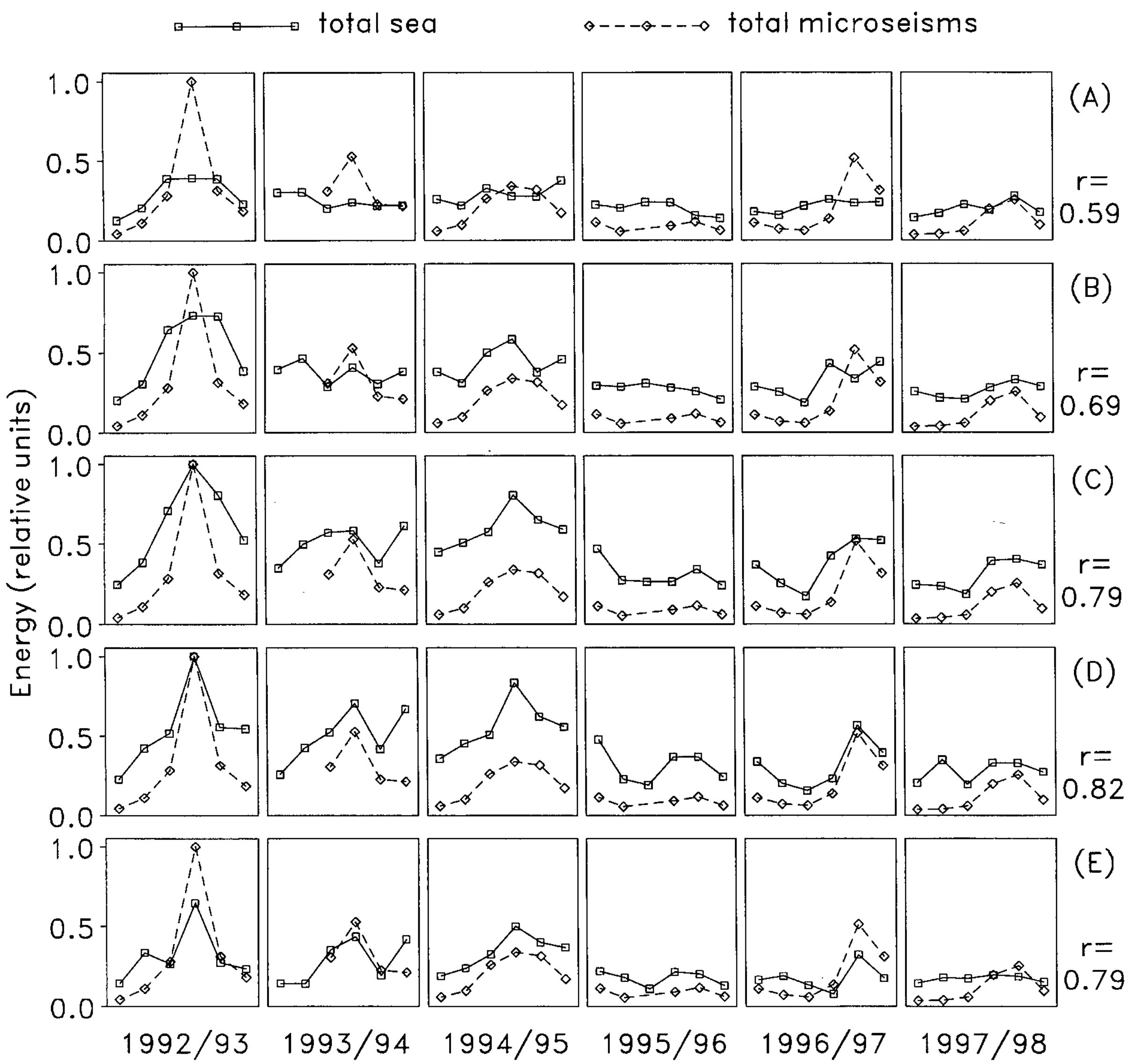

Fig. 5: Monthly means of ocean-wave and microseismic energy in the areas A - E along the Norwegian coast, cf. Fig. 1, for the six winters indicated. Energies are normalized to the maximum values of the total sea and the total microseisms, respectively. The correlation coefficient r refers to the six-winter time series.

Fig. 6 compares the 10 % percentile of the sample distribution of quadratic ocean-wave amplitudes with linear microseismic amplitudes. Considering quadratic or linear amplitudes for both the ocean waves and the microseisms somewhat smaller correlation coefficients were found. In most cases, the difference is less than 5 %. Dividing the sea state into wind sea and swell on the one hand and 6-s and 8-s microseisms on the other hand yields similar results as discussed in conjunction with Fig. 5, i.e., the comparison of mean energies. Particulary, the increased sensitivity of the 6-s microseisms to the sea state at the southern Norwegian coast is confirmed by correlation coefficients of $r = 0.85$ in area C, $r = 0.83$ in area D, and $r = 0.85$ in area E. Again, the comparison of the 10 % percentile of the wind speed (instead of the ocean-wave height) with that of the microseisms yields only sligthly smaller correlation coefficients.

Encouraged by the results presented we compared, directly, monthly means of microseisms with the monthly index of the winter NAO index. The NAO index is a measure of the strength of the atmospheric circulation above the North Atlantic. It is defined as the normalized mean atmospheric pressure difference between the Azores and Iceland (Rogers, 1984),

$$I_{NAO} = \left.\frac{p-\bar{p}}{\sigma}\right|_{Az} - \left.\frac{p-\bar{p}}{\sigma}\right|_{Ic} \tag{3}$$

where p denotes the (monthly mean) sea-level atmospheric pressure, $\bar{p}$ and σ its long-term mean and standard deviation, respectively. The monthly NAO index data used in this paper refer to the stations Ponta Delgada (Azores) and Reykjavik (Iceland) and are availabe since 1865. The data were obtained from the World Monthly Surface Station Climatology (http://www.scd.ucar.edu/dss/datasets/ds 570.0.html).

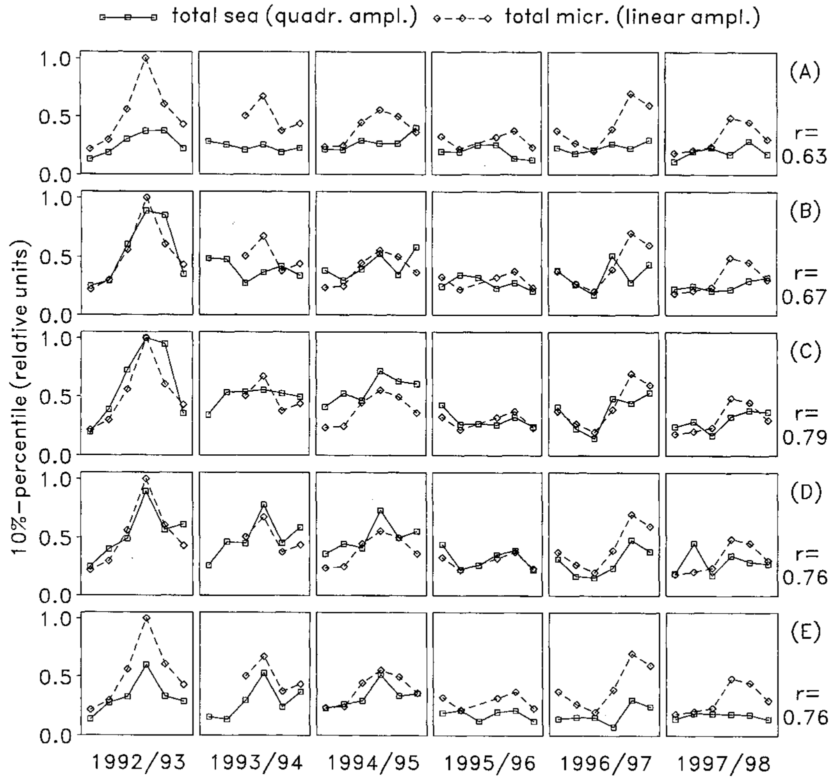

Fig. 6: 10% percentile of the sample distribution of quadratic ocean-wave amplitude (full lines) and linear microseismic amplitude (dashed lines) in the areas A - E along the Norwegian coast, cf. Fig. 1. Percentiles are normalized to the maximum values of the total sea and the total microseisms, respectively. The correlation coefficient r refers to the six-winter time series.

Fig. 7 compares the monthly winter NAO index with the average microseismic energy recorded in Hamburg. It turned out that by considering the microseismic energy instead of the amplitude the correlation coefficients increased by some 15%. The NAO index is only a very rough measure of the atmospheric circulation in the North Atlantic, because it gives no information about the position and size of low pressure regions. The NAO index, however, is related to the strength of the westerlies over the North Atlantic Ocean. Microseisms is generated by ocean waves which in turn are generated by wind. Thus, some correlation can be expected. As most of the microseisms is originated at the Norwegian coast, less correlation of microseisms is expected with the NAO index than with ocean-wave heights in selected areas.

Fig. 7 reveals correlation coefficients of the order of $r = 0.6$ of the monthly winter NAO index versus the microseismic energy in Hamburg. The 4-s is included in order to demonstrate its relatively low correlation. The 6-s microseisms are correlated somewhat better than the 8-s and total microseims. However, considering the 95 % confidence intervals, this difference is not statistically significant. The correlations found are in accordance with the former results and encourage to make use of the total microseismic amplitude for analysing historic microseismic recordings.

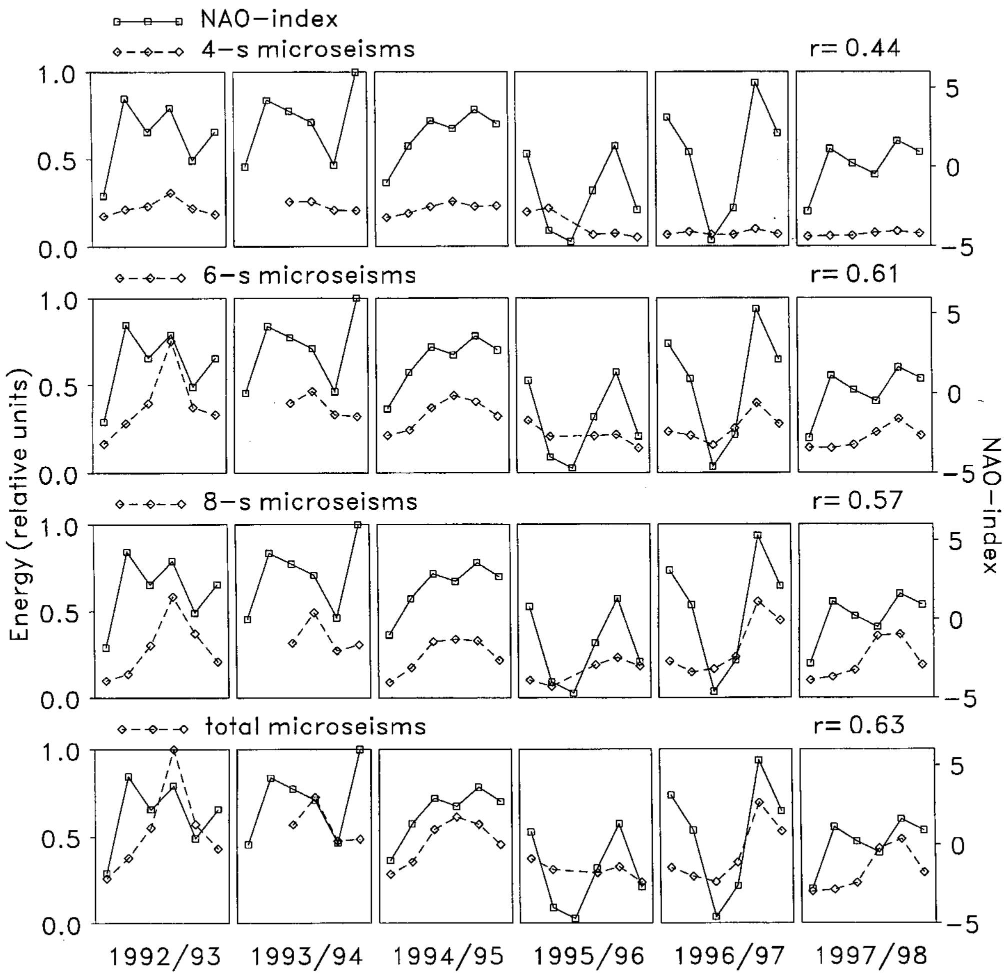

Fig. 7: Monthly means of microseismic energy at center frequencies of 4 s, 6 s and 8 s and total microseisms (from above) compared with the monthly index of the North Atlantic Oscillation (NAO). NAO-index and microseismic energy μm^2 are normalized to their maximum values. The correlation coefficient r refers to the six-winter time series.

5 Conclusions

Microseisms, recorded digitally in Hamburg (Germany) since 1992 is compared with modelled maps of the sea state in the North Atlantic. The correlation analysis reveals some evidence that the preferential generation areas of microseisms are the coast of southern Norway and the Atlantic coasts of Scotland and Ireland. Less correlation was found for areas in the open North Atlantic and for the North Sea. However, the emphasis of this paper is not on the detection of source areas but on the dependence of microseismic activity on climate variability. Considering 6-hourly sampled time series, a correlation coefficient of $r = 0.71$ was found by comparing the square-root amplitude of the microseisms with the mean ocean-wave height along the Norwegian coast. The ocean-wave data used are numerical predictions of the sea state. They may deviate from the real sea state during the microseismic recordings. Because of this error, it can be expected that the real correlation between microseisms and sea state is somewhat higher than found in our analysis.

Even higher correlation coefficients of up to $r = 0.85$ were found by comparing monthly means of ocean-wave and microseismic energy in selected areas. The 6-s microseisms are correlated more strongly with the sea state than the 8-s microseisms. A reason for this finding may be that secondary 8-s microseisms is generated by 16-s ocean waves (400 m wavelength), i.e. mainly by swell which represents only part of the sea state. Replacing ocean-wave height by wind speed in the correlation analysis, it turned out that in the case of 6-hourly sampled time series the correlation coefficients decrease by about 20 %, while for the time series of monthly means the decrease is of the order of 4 % only.

The high correlation between monthly means of microseismic and the ocean-wave energy, but also the wind energy, will allow for using historical microseismic recordings for estimating the frequency and strength of storm events in the past 100 years. SCHMIDT and VON STORCH (1993) analysed pressure records around the German Bight (southern North Sea) and concluded that the storm statistics of this area has not changed in the past 100 years. Our intention in investigating historical microseisms is to confirm or contradict this statement for an extended area in the North Atlantic.

Finally, the correlation coefficient of $r = 0.63$ confirms that microseisms can be added to the long list of geophysical parameters which are affected by the NAO index: latent and sensible heat flux over the North Atlantic (CAYAN [1992]), evaporation and precipation (HURRELL [1995]), deuterium in the Greenland ice sheet (BARLOW et al. [1993]), ice volume in the Baltic (KOSLOWSKI AND LOEWE [1994]), etc. The analysis presented is based on data from six winters only. Longer microseismic time series have to be analysed for resolving the decadal variability, though this work will be tedious as the historical microseisms is recorded on paper.

Acknowledgement

The Bundesamt für Seeschiffahrt und Hydrographie (BSH) provided the sea state data. We are grateful to D. Schrader (BSH) for preparing the data for our purposes. The index of the NAO was obtained from the World Monthly Surface Station Climatology (WWW page). The work was supported by the German Science Foundation (Deutsche Forschungs Gemeinschaft, DFG; Sonderforschungsbereich 512: Tiefdruckgebiete und Klimasystem des Nordatlantiks).

References

BARLOW, L. K., WHITE, J. W. C., BARRY, R. G., ROGERS, J. C., GROTTES, P. M., 1993: The North Atlantic Oscillation signature in deuterium and deuterium excess signals in the Greenland Ice Sheet Project-2. Ice Core, 1840-1970. *Geophys. Res. Letters,* **20**, 2901–2904.

BEHRENS, A. AND D. SCHRADER, 1994: The wave-forecast system of the 'Deutscher Wetterdienst' and the 'Bundesamt für Seeschiffahrt und Hydrographie': A verification using ERS-1 altimeter and scatterometer data. *Dt. hydrogr. Z.*, **46**, 131–149.

CAYAN, D. R, 1992: Latent and sensible heat flux anomalies over the northern oceans: The connection to monthly atmospheric oscillation. *J. Clim.*, **5**, 354–369.

FRIEDRICH, A., KRÜGER, F., KLINGE, K., 1998: Ocean-generated microseismic noise located with the Gräfenberg array. *Journ. of Seismol.* **2**, 47–64.

HASSELMANN, K. A., 1963: Statistical analysis of the generation of microseisms. *Reviews of Geophysics*, **1**, 177–210.

HURRELL, J. W., 1995: Decadal trends in the North Atlantic Oscillation: Regional temperatures and precipitation. *Science*, **269**, 676–679.

GÜNTHER, H., ROSENTHAL, W., WEARE, T. J., WORTHINGTON, B. A., HASSELMANN, K., EWING, J. A., 1979: A hybrid parametrical wave prediction model. *J. Geophys. Res.*, **84**, 5727–5738.

GUTENBERG, B., 1924: Die seismische Bodenunruhe. *Sammlung Geophysikalischer Schriften*, 3, 67 pp., Berlin: Bornträger.

KOSLOWSKI, G. AND P. LOEWE, 1994: The western Baltic sea ice season in terms of mass-related severity index: 1879–1992. Part I. Temporal variability and association with the North Atlantic Oscillation. *Tellus*, **46A**, 66–74.

LONGUETT-HIGGINS, M. S., 1950: A theory of the origin of microseisms. *Phil. Trans. Roy. Soc. London, Ser. A*, **243**, 1–35.

MICHE, M., 1944: Movements ondulatoires de la mer en profendeur constante ou decroissante. *Ann. Ponts Chaussees*, **114**, 25–87, 131–164, 270–292, 396–406.

ROGERS, J. C., 1984: The association between the North Atlantic Oscillation and the Southern Oscillation in the northern hemisphere. *Monthly Weather Review*, **12**, 1999–2015.

SCHMIDT, H. AND H. VON STORCH,1993: German Bight storms analysed. *Nature*, **365**, 791.

STROBACH, K., 1962: Ein Beitrag zum Problem der Entstehung und der Wellennatur der mikroseismischen Unruhe. *Hamburger Geophysikalische Einzelschriften*, 5, 125 pp.

STORCH, H. VON, ALEXANDERSSON, H., BOUWS, E., CARRETERO, J. C., GONZALEZ, I. L., GUDDAL, J., GÜNTHER, H., JANNINK, D., KHARIN, V., KOMEN, G., REICHARDT, H., ROSENTHAL, W., RUIZ DE ELVIRA, A., SCHMITH, T., STAWARZ, M., 1995: The WASA project: changing storm and wave climate in the Northeast Atlantic and adjacent seas? 4th International Workshop on Wave Hindcasting and Forecasting, Oct. 16–20, 1995, Banff (Canada), 31–44.

Submitted: 03.02.1999
Accepted: 22.09.1999

Addresses of authors:

H.-H. Essen
Institut für Meereskunde
Universität Hamburg
Troplowitzstr. 7
D- 22529 Hamburg

J. Klussmann
R. Herber
Institut für Geophysik
Universität Hamburg
Bundesstr. 55
D-20146 Hamburg

I. Grevemeyer
Fachbereich Geowissenschaften
Universität Bremen
Klagenfurter Str.
D-28359 Bremen